

Analysis of Phase Diagrams Employing Bayesian Excess Parameter Estimation**

Erich Königsberger and Heinz Gamsjäger*

Abteilung für Physikalische Chemie, Montanuniversität Leoben, A-8700 Leoben, Austria

Summary. Bayesian estimation of thermodynamic excess quantities was applied to liquidus data of the systems cyclohexane – benzene and potassium chloride – sodium chloride as well as data on the austenite \rightleftharpoons ferrite equilibrium of the iron – zinc system. Theoretical considerations (KCl – NaCl) and results from calorimetric or partial pressure studies (Fe – Zn) were used as independent *a priori* information. The recalculated phase diagrams coincide perfectly with those given in the literature. In each case the thermodynamic significance of the experimental data is discussed.

Keywords. Bayesian estimation; Phase diagrams; Thermodynamic functions.

Analyse von Phasendiagrammen unter Anwendung des Bayes-Verfahrens

Zusammenfassung. Zur Ermittlung von thermodynamischen Exzeß-Funktionen aus Liquidus-Daten der Systeme Cyclohexan – Benzol und Kaliumchlorid – Natriumchlorid sowie aus Daten für das Austenit \rightleftharpoons Ferrit-Gleichgewicht im System Eisen – Zink wurde das Bayes-Verfahren herangezogen. Ein theoretisches Modell (KCl – NaCl) und Ergebnisse von calorimetrischen bzw. Partialdruck-Messungen (Fe – Zn) wurden als unabhängige *a priori* Informationen verwendet. Die so berechneten Phasendiagramme fallen sehr genau mit den in der Literatur angegebenen zusammen. In jedem einzelnen Fall wird die thermodynamische Signifikanz der experimentellen Daten diskutiert.

Introduction

Nonlinear least-squares procedures are useful tools for the estimation of model parameters from experimental data. Often *a priori* information on these parameters is available from independent measurements or theoretical considerations. Whereas the conventional weighted least-squares algorithm takes only the experimental data into account, Bayesian estimation uses also additional information on the parameters sought for [1–3]. There are numerous applications of global and sequential Bayes algorithms in physics and astronomy, however, applications to chemical problems are rather scarce.

Some years ago Bayesian parameter estimation was employed for the determination of the three principal components of the molecular rotational diffusion

** Dedicated to Professor Erich Schwarz-Bergkampf on occasion of the 85th anniversary of his birthday

tensor from the time evolution of various magnetization modes measured by NMR relaxation [4–6].

Recently, a FORTRAN code IONLSQ 3 which allows the Bayesian estimation of complex formation constants has been written and applied to unravel the protolysis scheme of telluric acid in aqueous solutions [7]. Although numerous highly sophisticated computer programs for similar problems have recently been reviewed [8], it seems that *a priori* and experimental information have so far never simultaneously been used for the least-squares calculation of equilibrium constants.

The development of techniques to perform analyses coupling thermodynamic and phase diagram data is a subject of current interest which led to the publication of a special journal (CALPHAD). The Bayes method recommends itself for data fitting in this field, where *a priori* information is often available from independent sources, e.g., calorimetric, vapour pressure, mass spectrometric or e.m.f. measurements. In the present paper, a nonlinear Bayes algorithm is proposed for the estimation of excess parameters from experimental phase diagram data. Liquid-vapour (cyclohexane – benzene), solid-liquid (potassium chloride – sodium chloride) and solid-solid (iron – zinc) $T-x$ phase diagrams were selected as examples for its application.

Calculation Procedure

Bayesian Estimation

In general, a parameter estimation method involves defining an error function E which expresses the difference between the predicted and experimental data. The error function depends only on the parameters which are used for the mathematical definition of the chemical model. The task is then to find the model parameter values that correspond to a minimum of the error function. An important aspect of parameter estimation is to establish the uncertainties in experimental data as well as in original model parameters.

The error function in Bayesian estimation consists of two parts: (1) the difference between the predicted and experimental data; and (2) the difference between the original and final parameter values, i.e.

$$E(\mathbf{p}) = [\mathbf{f}(\mathbf{p}) - \mathbf{y}]^T \mathbf{C}_y^{-1} [\mathbf{f}(\mathbf{p}) - \mathbf{y}] + [\mathbf{p} - \mathbf{p}^0]^T \mathbf{C}_{p^0}^{-1} [\mathbf{p} - \mathbf{p}^0], \quad (1)$$

where \mathbf{p}^0 , \mathbf{y} and $\mathbf{f}(\mathbf{p})$ denote vectors of *a priori* parameters, experimental data and corresponding calculated values, respectively. \mathbf{C}_y and \mathbf{C}_{p^0} are covariance matrices of experimental function values and *a priori* parameters \mathbf{p}^0 , respectively. The inverse of \mathbf{C} equals the weighting matrix.

Thus, the two parts of the error function can be weighted differently depending on whether more confidence is placed in the experimental data or the original model properties.

It can be derived from the Newton-Raphson minimization method [9] that the normal equations for nonlinear Bayesian estimation become in matrix notation

$$\mathbf{p}^{(i+1)} - \mathbf{p}^{(i)} = [\mathbf{A}^T \mathbf{C}_y^{-1} \mathbf{A} + \mathbf{C}_{p^0}^{-1}]^{-1} \cdot [\mathbf{C}_{p^0}^{-1} [\mathbf{p}^0 - \mathbf{p}^{(i)}] + \mathbf{A}^T \mathbf{C}_y^{-1} [\mathbf{y} - \mathbf{f}(\mathbf{p}^{(i)})]], \quad (2)$$

where \mathbf{A} is given by $A_{jk} = \partial f_j(\mathbf{p}^{(0)}) / \partial p_k$. For the weighted least-squares algorithm $C_{\mathbf{p}^{(0)}}^{-1} = \mathbf{O}$. The iteration procedure is repeated until the parameter improvement is negligible.

Analysis of Phase Diagrams

From the equilibrium conditions at constant pressure (3)

$$\Delta_{\alpha}^{\beta} \mu_i^*(T) + RT \ln \frac{x_i^{\beta}}{x_i^{\alpha}} + \mu_i^{\text{E}(\beta)}(T) - \mu_i^{\text{E}(\alpha)}(T) = 0, \quad i = \text{A, B}, \quad (3)$$

the isobaric binary phase diagram $T - x^{\alpha} - x^{\beta}$ can be calculated if the various μ functions are known. The function $\Delta_{\alpha}^{\beta} \mu_i^*(T)$ refers to the $\alpha \rightarrow \beta$ phase transition of the pure component i . The excess chemical potentials

$$\mu_i^{\text{E}} = G^{\text{E}} + (1 - x_i) \frac{\partial G^{\text{E}}}{\partial x_i} \quad (4)$$

are related by Eq. (4) to the excess Gibbs function which is often written in Redlich-Kister form

$$G^{\text{E}} = x(1 - x)[G_1^{\text{E}} + G_2^{\text{E}}(1 - 2x) + G_3^{\text{E}}(1 - 2x)^2 + \dots] \quad (5)$$

or with orthogonal Legendre-polynomials [10]

$$G^{\text{E}} = x(1 - x)[G_1^{\text{E}} + G_2^{\text{E}}(2x - 1) + G_3^{\text{E}}(6x^2 - 6x + 1) + \dots], \quad (6)$$

where for the sake of brevity $x \equiv x_{\text{B}}$. Often the G_j^{E} -parameters may be written as a linear function of temperature

$$G_j^{\text{E}} = H_j^{\text{E}} - TS_j^{\text{E}}, \quad (7)$$

where H_j^{E} and S_j^{E} are excess enthalpy and entropy parameters, respectively.

Since the μ^{E} 's are linear functions of the excess parameters, the latter can be evaluated by linear least-squares methods provided the $\Delta_{\alpha}^{\beta} \mu^*$'s and experimental $T - x^{\alpha} - x^{\beta}$ data are known. Least-squares methods, e.g. [11, 12], have been described for optimizing simultaneously thermodynamic functions and phase diagrams from experimental data of both.

In the new approach excess parameters are estimated by a nonlinear Bayes algorithm. In Eq. (2) the vector \mathbf{y} refers to experimental phase diagram data $x(T)$, whereas $\mathbf{f}(\mathbf{p})$ is calculated iteratively from the equilibrium conditions (3). As indicated above, $\mathbf{f}(\mathbf{p})$ is a nonlinear function of the excess parameters \mathbf{p} . The vector \mathbf{p}^0 contains the thermodynamic excess parameters derived previously from independent measurements.

It should be emphasized that in this procedure measured and calculated x values are compared directly. This is advantageous when data for only one phase boundary have been experimentally determined. In this case, additional information on excess parameters is in general necessary [13]. Several other strategies to solve this problem have been proposed [13, 14]. However, the method described in this paper has some useful aspects which have not been exploited so far.

Results and Discussion

Liquid-Vapour Phase Diagram of Cyclohexane–Benzene

Precise determinations of isobaric $T - x^l - x^v$ data require special equilibrium stills and are experimentally rather demanding. At least for a first orientation, $T - x^l$ (boiling point) data can be obtained much more easily and rapidly.

Whereas for isothermal liquid-vapour equilibria $P - x^l$ (total pressure) evaluation methods are well-established [15], the situation is less favourable with $T - x^l$ data.

In this paper it is shown that liquidus points suffice to calculate the complete phase diagram of, e.g., cyclohexane-benzene which has been proposed as a test system for phase equilibrium and calorimetric measurements [16, 17].

Input data were $T - x^l$ values of the data set at 101.325 kPa recommended by

Table 1. Cyclohexane-benzene: excess parameters

j	<i>A priori</i> information		Bayesian estimation	
	$H_j^{E(l)}/\text{J mol}^{-1}$	$S_j^{E(l)}/\text{J mol}^{-1} \text{K}^{-1}$	$H_j^{E(l)}/\text{J mol}^{-1}$	$S_j^{E(l)}/\text{J mol}^{-1} \text{K}^{-1}$
1	2646.9 ± 37.0	4.39 ± 0.27	2631 ± 34	4.68 ± 0.10
2	-121.2 ± 60.0	0.19 ± 0.75	-115 ± 59	-0.11 ± 0.18
3	74.1 ± 151.0	0 ± 1.50	66 ± 145	0.27 ± 0.44

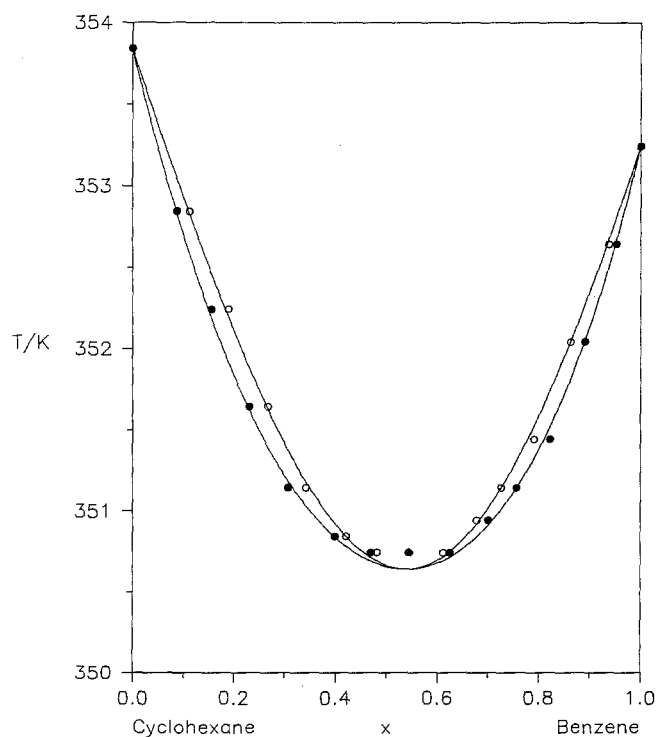


Fig. 1. Liquid-vapour phase diagram of cyclohexane–benzene: ● liquidus points [16] which have been used for the Bayesian estimation, ○ vaporus points [16]

Smith et al. [16], Table 16. The temperature dependence of the free enthalpies of evaporation were taken to be

$$(\mu_{\text{cyclohex.}}^{*v} - \mu_{\text{cyclohex.}}^{*l})/\text{kJ mol}^{-1} = 30.10(1 - T/353.85 \text{ K}), \quad (8)$$

$$(\mu_{\text{benzene}}^{*v} - \mu_{\text{benzene}}^{*l})/\text{kJ mol}^{-1} = 30.80(1 - T/353.25 \text{ K}). \quad (9)$$

When the vapour is treated as perfect gas Bayesian parameter estimation for the function (10),

$$\begin{aligned} G^{\text{E}(l)} = & x(1-x)[(H_1^{\text{E}(l)} - TS_1^{\text{E}(l)} \\ & + (H_2^{\text{E}(l)} - TS_2^{\text{E}(l)})(1-2x) \\ & + (H_3^{\text{E}(l)} - TS_3^{\text{E}(l)})(1-2x)^2] \end{aligned} \quad (10)$$

leads to the results presented in Table 1. $H^{\text{E}(l)}$ at 348.15 K [18] is used as *a priori* information. Fitting the data of Ref. [18], Table 3 results in the function

$$\begin{aligned} H^{\text{E}(l)} = & x(1-x)[(2646.9 \pm 3.7) + (-121.2 \pm 6.0)(1-2x) \\ & + (74.1 \pm 15.1)(1-2x)^2] \text{ J mol}^{-1}. \end{aligned}$$

In addition, *a priori* S_j^{E} parameters were estimated from selected $G^{\text{E}}(T)$ values (Ref. [16], Table 9). The *a priori* uncertainties ascribed to these parameters were chosen ten times the uncertainties derived from the original measurements [18], in order to put more weight on the boiling point data. However, the input parameters were hardly altered at all. This and the large uncertainties indicate that the pertinent phase diagram data can be explained by a simpler model, like that of Chao and Hougen [19].

The phase diagram corresponding to the excess parameters of Table 1 is depicted in Fig. 1. Although the experimental vaporus points have not been included in the least-squares analysis they lie within a narrow range of the curve calculated.

T-x Phase Diagram in the System KCl-NaCl

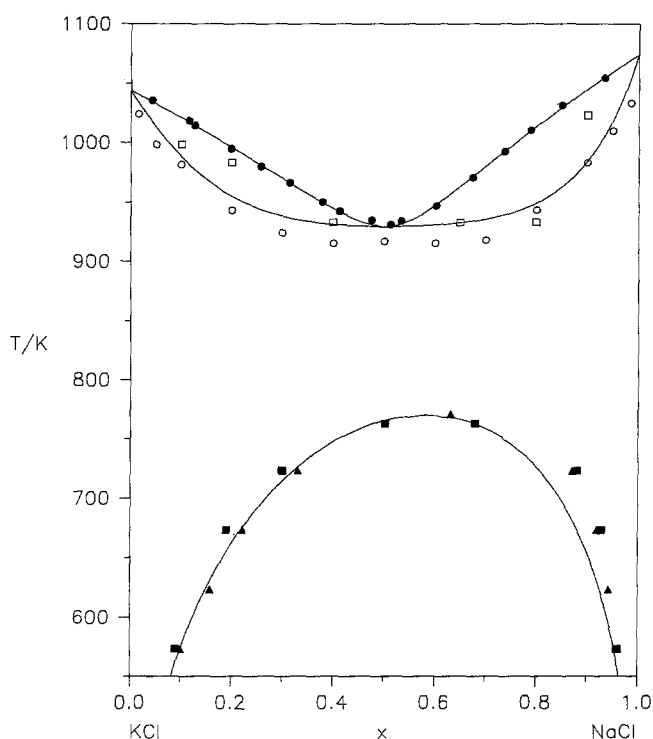
A solid-state chemical model which predicts enthalpies of mixing [20] and $T-x$ phase diagrams [21] of binary alkali halide systems with a range of complete solid miscibility has recently been proposed. The excess Gibbs enthalpy $G^{\text{E}(s)}$ is given by Eq. (11),

$$G^{\text{E}(s)} = 1600x(1-x)[(1-x)\Delta_{\text{KCl}}^2 + x\Delta_{\text{NaCl}}^2](1 - T/2100 \text{ K}) \text{ kJ mol}^{-1}, \quad (11)$$

where $\Delta_i = (r_i - r_k)/r_i$ and the r_i 's denote the nearest-neighbour distances of the pure component i . The quantities $H_j^{\text{E}(s)}$ and $S_j^{\text{E}(s)}$ calculated from this model and $H_j^{\text{E}(l)}$ measured calorimetrically [22] were used as *a priori* parameters, whereas liquidus points from the most recent study [23] were employed as experimental input data. Values for $(\mu_{\text{KCl}}^{*l} - \mu_{\text{KCl}}^{*s})$ and $(\mu_{\text{NaCl}}^{*l} - \mu_{\text{NaCl}}^{*s})$ have also been taken from Pelton et al. [23]. As shown in Fig. 2, the so calculated liquidus, solidus and region of demixing curves agree very well with experimental data. In a first run it turned out that uncertainties larger than the values were ascribed to $S_j^{\text{E}(l)}$. Consequently, these parameters were omitted in the final evaluation. As may be seen in Table 2, the *a priori* quantities have been altered only slightly by the least-squares procedure,

Table 2. KCl–NaCl: excess parameters

Thermodynamic parameters	<i>A priori</i> information	Bayesian estimation I	Bayesian estimation II
$H_1^{E(l)}/\text{J mol}^{-1}$	-2186 ± 1000	-2160 ± 540	-2190 ± 390
$S_1^{E(l)}/\text{J mol}^{-1} \text{K}^{-1}$	—	0.023 ± 0.454	—
$H_2^{E(l)}/\text{J mol}^{-1}$	136 ± 500	390 ± 370	560 ± 240
$S_2^{E(l)}/\text{J mol}^{-1} \text{K}^{-1}$	—	-0.23 ± 0.38	—
$H_1^{E(s)}/\text{J mol}^{-1}$	19870 ± 400	19770 ± 380	19760 ± 370
$S_1^{E(s)}/\text{J mol}^{-1} \text{K}^{-1}$	9.46 ± 0.30	9.51 ± 0.29	9.51 ± 0.29
$H_2^{E(s)}/\text{J mol}^{-1}$	-2200 ± 200	-2230 ± 200	-2250 ± 190
$S_2^{E(s)}/\text{J mol}^{-1} \text{K}^{-1}$	-1.05 ± 0.30	-0.99 ± 0.29	-0.95 ± 0.28

**Fig. 2.** Phase diagram of the KCl–NaCl system: ● liquidus points [23] which have been used for the Bayesian estimation, □ [28] and ○ [29] solidus points, ■ [30] and ▲ [31] region of solid demixing

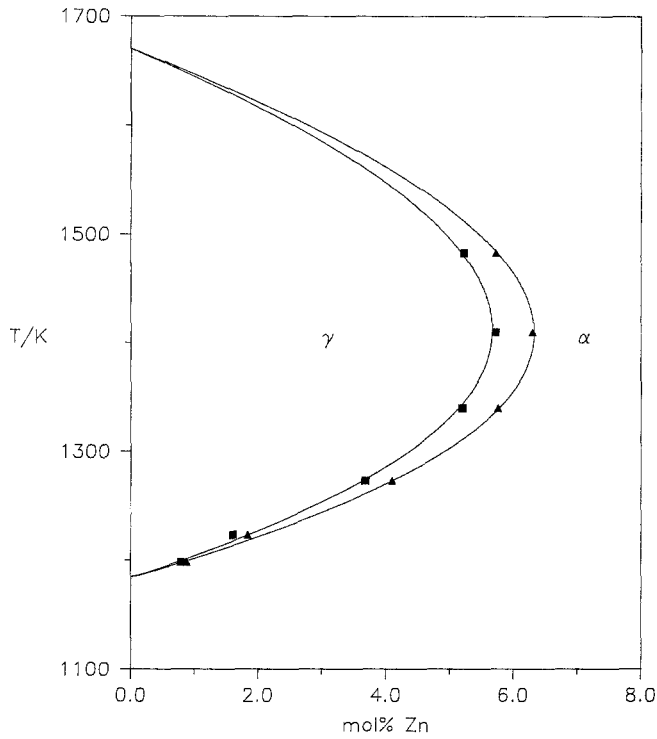
thus the solid-state chemical model of alkali halide mixtures [20, 21] is consistent with the present analysis.

The γ Loop in the System Fe–Zn

Kirchner et al. [24] determined the saturation contents of zinc in ferrite (α -phase) and austenite (γ -phase) carefully by means of the microprobe. For the analysis of these data and the synthesis of the respective T – x phase diagram additional thermodynamic information on the α -phase is available [25]. The partial pressure of zinc in equilibrium with ferrite has been measured and interpreted by an asym-

Table 3. Fe–Zn: excess parameters

Thermodynamic parameters	<i>A priori</i> information	Bayesian estimation
$H_1^{E(\alpha)}/\text{J mol}^{-1}$	4390 ± 270	4440 ± 250
$S_1^{E(\alpha)}/\text{J mol}^{-1} \text{K}^{-1}$	-6.27 ± 0.73	-6.12 ± 0.54
$H_2^{E(\alpha)}/\text{J mol}^{-1}$	4440 ± 270	4310 ± 230
$H_1^{E(\gamma)}/\text{J mol}^{-1}$	—	6610 ± 320
$S_1^{E(\gamma)}/\text{J mol}^{-1} \text{K}^{-1}$	—	-5.12 ± 0.54
$H_2^{E(\gamma)}/\text{J mol}^{-1}$	—	4590 ± 270

**Fig. 3.** The γ -loop in the Fe–Zn system: ■ and ▲ refer to austenite and ferrite, respectively [24]

metric mixing model [24]. For pure iron a regression analysis of data given by Harvig [26] resulted in Eq. (12) for the range between $1184.5 \leq T/\text{K} \leq 1668.1$,

$$\begin{aligned}
 (\mu_{\text{Fe}}^{*\alpha} - \mu_{\text{Fe}}^{*\gamma})/\text{J mol}^{-1} = & -8642.21 + 69.1650 T/\text{K} \\
 & -9.08670 (T/\text{K}) \ln (T/\text{K}) \\
 & + 2.05898 \times 10^{-3} (T/\text{K})^2. \quad (12)
 \end{aligned}$$

According to Kaufman [27] the temperature dependence of $\mu_{\text{Zn}}^{*\alpha} - \mu_{\text{Zn}}^{*\gamma}$ can be calculated by Eq. (13),

$$(\mu_{\text{Zn}}^{*\alpha} - \mu_{\text{Zn}}^{*\gamma})/\text{J mol}^{-1} = 1046 - 0.8368 T/\text{K}. \quad (13)$$

Now, in the nonlinear Bayesian estimation numerical values of $H_1^{E(\alpha)}$, $S_1^{E(\alpha)}$ and $H_2^{E(\alpha)}$ as suggested by Kirchner et al. [24] have been taken as *a priori* information.

The $T-x$ diagram of Fig. 3 was plotted with the estimated quantities listed in Table 3. The experimental x -values coincide almost precisely with the calculated curve. It was no longer necessary to invoke the approximations employed previously ($H_2^{E(\gamma)} = H_2^{E(\alpha)}$ and $G^\gamma = G^\alpha$ at $x_0 = (x_\gamma + x_\alpha)/2$). The results confirm the thermodynamic analysis of Kirchner et al. [24], whose approximations are indeed closely satisfied.

Conclusion

1. The simultaneous evaluation of experimental and *a priori* information, where different weights can be ascribed to either data set, makes Bayesian estimation a statistically powerful tool.
2. The Bayes method improves convergence [9] and ensures that physically reasonable quantities are selected for curve fitting.
3. When it is applied for the evaluation of thermodynamic quantities from phase diagrams the respective uncertainties can be estimated realistically, an aspect often neglected in current literature.

References

- [1] Box G. E. P., Tiao G. C. (1973) Bayesian Inference in Statistical Analysis. Addison-Wesley, Reading, MA
- [2] Sorenson H. W. (1980) Parameter Estimation. Marcel Dekker, New York
- [3] Sage A. P., Melsa J. L. (1971) Estimation Theory with Applications to Communication and Control. McGraw-Hill, New York
- [4] Königsberger E. (1985) Thesis. Karl-Franzens-Universität, Graz, Austria
- [5] Königsberger E., Sterk H. (1985) J. Chem. Phys. **83**: 2723
- [6] Sterk H., Königsberger E. (1986) J. Phys. Chem. **90**: 916
- [7] Königsberger E. (unpublished)
- [8] Meloun M., Havel J., Högfeldt H. (1988) Computation of Solution Equilibria. Wiley, New York
- [9] Walton W. B. (1989) Math. Comp. Modell. **12**: 181
- [10] Bale C. W., Pelton A. D. (1974) Metall. Trans. **5**: 2323
- [11] Lukas H. L., Henig E. T., Zimmermann B. (1977) CALPHAD **1**: 225
- [12] Bale C. W., Pelton A. D. (1983) Metall. Trans. **14B**: 77
- [13] Kohler H., Pelton A. D. (1982) CALPHAD **6**: 39
- [14] Van Genderen A. C. G., Bouwstra J. A., Brouwer N., Oonk H. A. J. (1980) Thermochim. Acta **38**: 97
- [15] Barker J. A. (1953) Aust. J. Chem. **6**: 207
- [16] Smith B. D., Muthu O., Dewan A., Gierlach M. (1982) J. Phys. Chem. Ref. Data **11**: 1099
- [17] Smith B. D., Muthu O., Dewan A., Gierlach M. (1982) J. Phys. Chem. Ref. Data **11**: 1127
- [18] Elliott K., Wormald C. J. (1976) J. Chem. Thermodynamics **8**: 881
- [19] Chao K. C., Hougen O. A. (1958) Chem. Eng. Sci. **7**: 246
- [20] Königsberger E., Schrunner H. (1989) Phys. Stat. Sol. (b) **151**: 101
- [21] Königsberger E. (accepted) Prediction of Phase Diagrams from Simple Mixing Models. Binary Alkali Halide Systems. Z. Phys. Chem. (Leipzig)
- [22] Hersh L. S., Kleppa O. J. (1965) J. Chem. Phys. **42**: 1309
- [23] Pelton A. D., Gabriel A., Sangster J. (1985) J. Chem. Soc., Faraday Trans. 1 **81**: 1167
- [24] Kirchner G., Harvig H., Moquist K. R., Hillert M. (1973) Arch. Eisenhüttenwes. **44**: 227
- [25] Wriedt H. A. (1967) Trans. Metallurg. Soc. AIME **239**: 1120

- [26] Harvig H. (1971) *Jernkont. Ann.* **155**: 157
- [27] Kaufmann L. (1959) *Bull. Am. Phys. Soc.* **4**: 181
- [28] Abramov G. A. (1935) *Metallurgia* **10**: 82
- [29] Coleman D. S., Lacy P. D. A. (1967) *Mater. Res. Bull* **2**: 935
- [30] Vesnin Y. I., Zakovryashin S. P. (1979) *Solid State Commun.* **31**: 635
- [31] Nguyen-Ba-Chanh (1964) *J. Chim. Phys.* **61**: 1428

Received September 30, 1989. Accepted November 7, 1989